Supporting Information

Improved H-adsorption ability of Cu in CuNi alloy nanodots toward the efficient photocatalytic H_2-evolution activity of TiO_2

Meiya Wang, [a] Ping Wang, [a*] Haoyu Long, [a] Xuefei Wang, [a] FengChen, [a] Huogen Yu[a,b*]

[a] School of Materials Science and Engineering, and School of Chemistry, Chemical Engineering and Life Sciences, Wuhan University of Technology, Wuhan 430070, PR China

[b] Laboratory of Solar Fuel, Faculty of Materials Science and Chemistry, China University of Geosciences, Wuhan, 430074, PR China

*Corresponding authors. Tel: +86(27)87749379;

E-mail: wangping0904@whut.edu.cn (Ping Wang);

huogenyu@163.com (Huogen Yu)

SI-1 Materials

Commercial Degussa TiO_2 nanoparticles (P25), $CuCl_2 \cdot 2H_2O$, $NiCl_2 \cdot 6H_2O$, and C_2H_5OH came from Shanghai Chemical Reagent Ltd. and anatase TiO_2 (25 nm) came from Shanghai Macklin Biochemical Co., Ltd. GO was prepared via a similar method to Hummer's consisted with our prior study [33].

SI-2 Characterization

The transmission electron microscope (TEM) (JEM-2100F, JEOL, Japan), X-ray diffractometer (XRD) (Rigaku, D/MX- IIIA, Japan), Raman microscope (In Via, Renishaw, UK), X-ray photoelectron spectroscopy (XPS) (Thermo Fisher, ESCALAB 250Xi, USA), UV-vis spectrophotometer (UV-2450, Shimadzu, Japan), and *in-situ* X-ray photoelectron spectrometer (ESCALAB 210, VG Scientific, UK) were used to confirm the microstructures of the as-prepared samples. The practical proportion of Cu and Ni in the samples was detected by the inductively coupled plasma optical emission spectrometer (ICP-OES) (Prodigy 7, LEEMAN LABS, USA).

SI-3 Photocatalytic H_2-evolution measurement

The photocatalytic system (prepared photocatalysts in ethanol solution) (Section 2) was directly applied in photocatalytic H_2-generation tests. Briefly, the above suspension was purged with nitrogen for 15 min to remove extra gases, then directly radiated by a 365 nm-LED lamp (150 W) to generate H_2. After irradiation for 1 h, 0.4 mL of gas was detected by a gas chromatograph (Shimadzu GC-2014C, Japan, with nitrogen as carrier gas) equipped with a 5 Å molecular sieve column and a thermal

conductivity detector every hour intervals during another 3 hours irradiation. Finally, the H_2-evolution rate was obtained by fitting the measured hydrogen-peak data. The corresponding apparent quantum efficiency (AQE) was calculated with the following equation:

$$\begin{aligned} \mathrm{AQE}(\%) &= \frac{\text{number of reacted electrons}}{\text{number of incident photons}} \times 100 \\ &= \frac{\text{number of evolved } H_2 \text{ molecules} \times 2}{\text{number of incident photons}} \times 100 \end{aligned} \tag{S1}$$

SI-4 Photoelectrochemical measurements

All photoelectrochemical properties are measured on a CHI660E electrochemical workstation (Chenhua Instrument, China) in a three-electrode configuration cell using Ag/AgCl, as-prepared sample-modified FTO glass, and Pt wire under the Na_2SO_4 solution (0.5 mol L^{-1}). The preparation of the working electrode referred to our previous work.**R[2]** Linear sweep voltammogram (LSV) curves were collected in the potential range from -0.8 V to -1.3 V at a scan rate of 10 mV s^{-1}. Transient photocurrent responses with time (*i-t*) curves were detected at 0.5 V bias potential under 3W-LED (365 nm). The electrochemical impedance spectroscopy (EIS) data were fitted according to those at open-circuit voltage with a frequency range of 10^{-3}-10^{6} Hz and an ac amplitude of 10 mV.

SI-5 DFT computational methods

The first principle calculation were carried out by using the Vienna Ab initio Simulation Package (VASP). Generalized gradient approximation (GGA) with

Perdew-Burke-Ernzerhof (PBE) functional was selected to describe the exchange-correlation interaction. The energy cutoff and Monkhorst-Pack k-point meshes were set as 450 eV and 3 × 3 × 1, respectively. The convergence threshold was set as 10^{-5} eV for energy and 0.01 eV·$Å^{-1}$ for force. To eliminate interactions between periodic structures, a vacuum of 20 Å was added. The Gibbs free energy of H atom adsorption (ΔG_{H*}) was defined as following equation:

$$\Delta G_H = \Delta E_H + \Delta E_{ZPE} - T\Delta S_H \tag{S2}$$

where ΔE_H, ΔE_{ZPE}, $T\Delta S_H$ are the differential hydrogen ΔE_H adsorption energy, the change in zero point energy and entropy between the adsorbed hydrogen and molecular hydrogen in gas phase, respectively, and T is the temperature. The term $T\Delta S_H$ was calculated to be -0.2 eV. To simulate the alloy structure of CuNi, the CuNi alloy model was constructed by replacing one Cu atom with one Ni atom on (100) facet of Cu.

Figure captions

Fig. S1. The photocatalytic H_2-evolution rate of CuNi-rGO/TiO_2 photocatalyst in (a) ethanol solution (25 vol%) and (b) pure water.

Fig. S2. The photocatalytic H_2-evolution rate of CuNi-rGO/TiO_2 photocatalyst under (a) 365 nm and (b) 420 nm wavelength.

Fig. S3. The photocatalytic H_2-evolution rate of (a) TiO_2(P25), (a') CuNi-rGO/TiO_2, (b) anatase TiO_2, (b') CuNi-rGO/anatase TiO_2, (c) CdS, and (c') CuNi-rGO/CdS.

Table S1. The application of rGO and metal in the field of photocatalysis.

Photocatalyst	Method	Light source	Sacrificial agent	H_2-production rate (mmol $h^{-1}g^{-1}$)	Ref.
TiO_2-rGO-Pt	photodeposition	mecury-vapor lamp (450 W)	methanol (10 vol%)	567	15
Au-TiO_2-rGO	hydrothermal	LED (3W)	methanol (25 vol%)	0.30	16
Au-Pd/rGO/TiO_2	hydrothermal	Xe (300 W)	methanol (25 vol%)	0.50	17
Pt-rGO-TiO_2	hydrothermal	PL-S (9W)	methanol (20 vol%)	0.51 (16 times)	R1
P25-rGO-Co	hydrothermal	mercury lamp (250 W)	methanol (20 vol%)	3.80 (32 times)	R2
Pt-GN-TiO_2	photodeposition	mecury-vapor lamp (8 W)	methanol (10 vol%)	6.58	R3
Pt-RGO/TiO_2	photodeposition	Xe (500 W)	methanol (25 vol%)	0.88 (1.6 times)	R4
Pt-RGO-TiO_2	hydrothermal photodeposition	mercury lamp (8 W)	methanol (10 vol%)	1.99	R5
Sr^{2+}/Ag-TiO_2@rGO	hydrothermal	Xe (250 W)	TEOA (10 vol%)	0.64	R6
CuNi-rGO/TiO_2	photodeposition	LED (150 W)	ethanol (25 vol%)	10.41 (53.7 times)	This work

15. M. A. Esteves, F. Fresno, V. R. Fernandes, F. E. Oropeza, V. A. de la Peña O'Shea and C. M. Rangel, *Catal. Today*, 2021, 380, 41-52.

16. Y. Wang, J. Yu, W. Xiao and Q. Li, *J. Mater. Chem. A*, 2014, 2, 3847-3855.

17. B. Tudu, N. Nalajala, P. R. K, P. Saikia and C. S. Gopinath, *ACS Appl. Mater. Interfaces*, 2019, 11, 32869-32878.

R1. M. J. Rivero, O. Iglesias, P. Ribao and I. Ortiz, *Int. J. Hydrogen Energy*, 2019, 44, 101-109.

R2. S. Min, F. Wang and G. Lu, *Catal. Commun.*, 2016, 80, 28-32.

R3. N. T. Nguyen, D. D. Zheng, S. S. Chen and C. T. Chang, *J Nanosci Nano.,* 2018, 18, 48-55.

R4. H. Li and X. Cui, *Int. J. Hydrogen Energy*, 2014, 39, 19877-19886.

R5. Y. Shinde, S. Wadhai, A. Ponkshe, S. Kapoor and P. Thakur, *Int. J. Hydrogen Energy*, 2018, 43, 4015-4027.

R6. X. Wei, J. Cao and F. Fang, *RSC Adv*, 2018, 8, 31822-31829.

Table S2. The ICP-OES results of the CuNi-rGO/TiO_2 samples.

Samples	Cu (wt%)	Ni (wt%)	Actual molar ratio of Cu to Ni	Actual molar ratio of CuNi to TiO_2 (at%)	Actual ratio of CuNi toTiO_2 (wt%)
CuNi-rGO/TiO_2 (1 wt%)	0.043	0.003	15	0.165	0.13
CuNi-rGO/TiO_2 (5 wt%)	1.114	0.059	17	1.514	1.2

Table S3. The photocatalytic H_2-evolution rate and apparent quantum efficiency (AQE) of various samples.

Samples	H_2 evolution rate ($\mu mol\ h^{-1}\ g^{-1}$)	AQE (%)
TiO_2	194	0.08
rGO/TiO_2	269	0.11
Cu-rGO/TiO_2	5924	2.50
CuNi-rGO/TiO_2(1:4)	7492	3.16
CuNi-rGO/TiO_2(2:3) (CuNi-rGO/TiO_2)	10411	4.39
CuNi-rGO/TiO_2(3:2)	7651	3.23
CuNi-rGO/TiO_2(4:1)	6372	2.69
Ni-rGO/TiO_2	4673	1.97

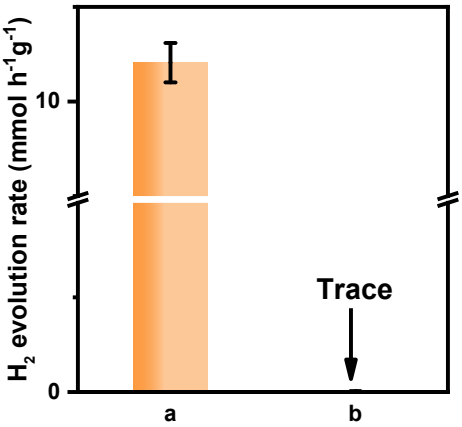

Fig. S1. The photocatalytic H_2-evolution rate of CuNi-rGO/TiO_2 photocatalyst in (a) ethanol solution (25 vol%) and (b) pure water.

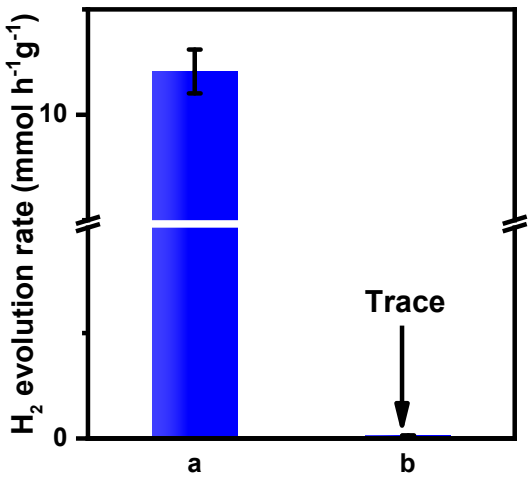

Fig. S2. The photocatalytic H_2-evolution rate of CuNi-rGO/TiO_2 photocatalyst under (a) 365 nm and (b) 420 nm wavelength.

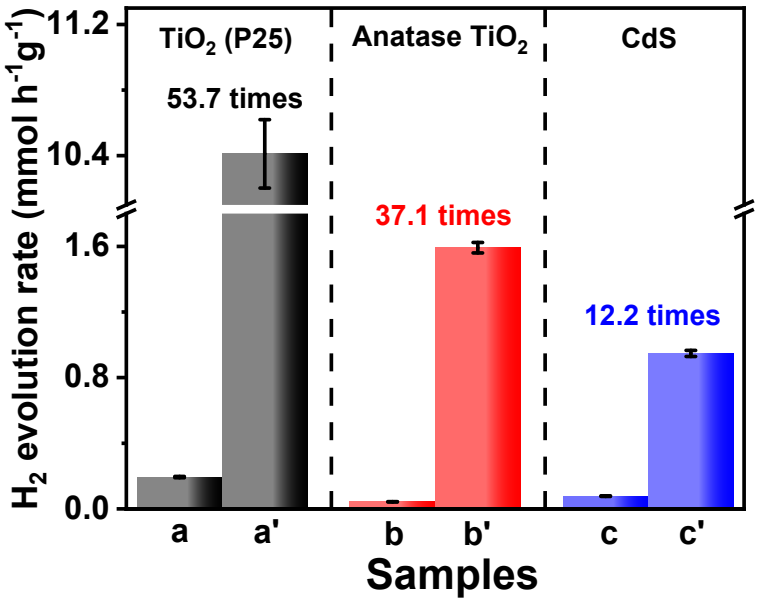

Fig. S3. The photocatalytic H_2-evolution rate of (a) TiO_2(P25), (a') CuNi-rGO/TiO_2, (b) anatase TiO_2, (b') CuNi-rGO/anatase TiO_2, (c) CdS, and (c') CuNi-rGO/CdS.